TECHNICAL REPORT BRL-TR-2956

BRL

1938 – Serving the Army for Fifty Years – 1988

BEAM ENVELOPE, INJECTION AND ACCELERATION IN A COMPACT, HIGH CURRENT, STRONG FOCUSED RECIRCULATING ACCELERATOR SCHEME

ANAND PRAKASH

DECEMBER 1988

U.S. ARMY LABORATORY COMMAND

BALLISTIC RESEARCH LABORATORY

ABERDEEN PROVING GROUND, MARYLAND

UNCLASSIFIED
SECURITY CLASSIFICATION OF THIS PAGE

REPORT DOCUMENTATION PAGE

Form Approved
OMB No. 0704-0188

1a. REPORT SECURITY CLASSIFICATION Unclassified	1b. RESTRICTIVE MARKINGS NA
2a. SECURITY CLASSIFICATION AUTHORITY NA	3. DISTRIBUTION/AVAILABILITY OF REPORT APPROVED FOR PUBLIC RELEASE; DISTRIBUTION UNLIMITED
2b. DECLASSIFICATION/DOWNGRADING SCHEDULE NA	
4. PERFORMING ORGANIZATION REPORT NUMBER(S) BRL-TR-2956	5. MONITORING ORGANIZATION REPORT NUMBER(S)
6a. NAME OF PERFORMING ORGANIZATION US Army Ballistic Research Laboratory 6b. OFFICE SYMBOL (If applicable) SLCBR-TB-EP	7a. NAME OF MONITORING ORGANIZATION
6c. ADDRESS (City, State, and ZIP Code) Aberdeen Proving Ground, MD 21005-5066	7b. ADDRESS (City, State, and ZIP Code)
8a. NAME OF FUNDING/SPONSORING ORGANIZATION US Army Ballistic Research Laboratory 8b. OFFICE SYMBOL (If applicable) SLCBR-D	9. PROCUREMENT INSTRUMENT IDENTIFICATION NUMBER
8c. ADDRESS (City, State, and ZIP Code) Aberdeen Proving Ground, MD 21005-5066	10. SOURCE OF FUNDING NUMBERS PROGRAM ELEMENT NO. 62618A; PROJECT NO. AH80; TASK NO. 00; WORK UNIT ACCESSION NO. 001AJ

11. TITLE (Include Security Classification)
(U) BEAM ENVELOPE, INJECTION AND ACCELERATION IN A COMPACT, HIGH CURRENT, STRONG FOCUSED RECIRCULATING ACCELERATION SCHEME

12. PERSONAL AUTHOR(S)
Anand Prakash

13a. TYPE OF REPORT	13b. TIME COVERED FROM ____ TO ____	14. DATE OF REPORT (Year, Month, Day)	15. PAGE COUNT

16. SUPPLEMENTARY NOTATION

17. COSATI CODES			18. SUBJECT TERMS (Continue on reverse if necessary and identify by block number)
FIELD	GROUP	SUB-GROUP	
20	07		accelerator, electrons, high-current, induction accelerator, recirculating accelerator; stellarator; strong focusing, torsatron, injection, beam envelope, electron beam, compact,
	09		

19. ABSTRACT (Continue on reverse if necessary and identify by block number)

In order to meet the criterion of compactness in developing high current, high energy electron accelerators, it is advantageous to recirculate the electron beam through an accelerating module. Various such recirculating accelerator concepts that use strong focusing magnetic fields may be conveniently referred to as SFRA ("Strong Focused Recirculating Accelerators"). The strong focusing field can be produced by external current carrying stellarator or torsatron windings. SLIA, Stellatron, RIA and rebatron are examples of SFRA.

High current electron beam transport in externally applied stellarator and longitudinal magnetic fields is analyzed. It is shown that a constant of motion exists for a matched beam of rotating elliptical cross-section, with self-fields included.
(Continued on back)

20. DISTRIBUTION/AVAILABILITY OF ABSTRACT	21. ABSTRACT SECURITY CLASSIFICATION
☒ UNCLASSIFIED/UNLIMITED ☐ SAME AS RPT ☐ DTIC USERS	Unclassified

22a. NAME OF RESPONSIBLE INDIVIDUAL	22b. TELEPHONE (Include Area Code)	22c. OFFICE SYMBOL
Anand Prakash	(301) 278-5680	SLCBR-TB-EP

DD Form 1473, JUN 86 — Previous editions are obsolete. — SECURITY CLASSIFICATION OF THIS PAGE

19. (Cont'd from front)

A differential equation for the beam envelope is derived and is shown to reduce to the familiar beam envelope equation for a beam of circular cross-section when the stellarator field is turned off.

A summary description of beam dynamics of acceleration in one SFRA, the rebatron, is given. Although a rebatron with major radius 100 cm and minor radius 10 cm can accelerate electrons to $\gamma \sim 65$ with a fixed vertical (bending) magnetic field, the insensitivity to energy mismatch poses a problem for beam trapping and injection. It is shown that a beam trapping scheme, in which a rapidly varying vertical magnetic field is applied before activating the rebatron acceleration gap, would work for a 10 kA beam of 1 cm radius injected near the wall of a rebatron of minor radius 16 cm.

TABLE OF CONTENTS

		Page
	LIST OF FIGURES	v
I	INTRODUCTION	1
II	AN ANALYSIS OF BEAM ENVELOPE IN STELLARATOR FIELDS	3
	A. Proof of a Constant of Motion	3
	B. Beam Envelope Equation	5
III	BEAM ACCELERATION AND INJECTION IN A REBATRON	8
	A. The Rebatron	8
	B. Beam Dynamics of Acceleration	11
	C. Beam Dynamics of Injection	19
IV	SUMMARY AND CONCLUSIONS	22
	REFERENCES	25
	DISTRIBUTION LIST	27

FIGURES

		Page
Figure 1.	Schematic of a SFRA named "rebatron". Inset at lower right shows low inductance coaxial lines to produce a vertical magnetic field that can be ramped.	9
2.	Schematic of the SFRA (strong focused recirculating accelerator) in which radial line/ET-2 cavities are used for producing electric field at the accelerating gap.	10
3.	Coordinate system used to study SFRA beam dynamics.	12
4.	(a) Electron energy [$\gamma \cong 2$ E (MeV)] as a function of time and (b) the corresponding particle orbit in the (r,z) plane, when the vertical field is held constant at 118 G in the SFRA shown in Figure 2.	16
5.	(a) Particle orbit in the transverse plane and (b) particle energy [$\gamma \cong 2$E (MeV)] as function of time in a rebatron, which has a rapidly increasing vertical field.	17
6.	Beam injected near the pipe wall (r = 114 cm) in a rebatron is brought to the center of the pipe (r = 100 cm) by applying a trapping field at injection.	20
7.	Variation of beam γ as a function of time after injection as the beam bounces toward the minor axis after injection near the wall for the case shown in Fig. 6.	21

I. INTRODUCTION

High current electron beam accelerators have become an active area of research because of their range of applications. The potential defense applications include particle beam weapons, flash radiography, nuclear effects simulation, and free electron lasers. The non-defense applications concern inertial fusion, nuclear waste transmutation and radioactive processing of food and sludge. Research at the Ballistic Research Laboratory (BRL) has been directed towards development of compact devices because of transportability requirements. For example, a compact radiographic device would be useful for on-site assessment of ballistic damage as well as for non-destructive testing of structural faults in equipment.

Induction accelerators--in which the acceleration is by an inductive electric field produced by a time-varying magnetic field--being inherently low-impedance devices, are naturally suited to drive high current beams. There are two generic types of high-current induction accelerators: *linear* (*e.g.* the ATA[1] at Livermore and the RADLAC[2] at Sandia), in which the accelerating field is localized in a series of accelerating gaps, and the cyclic (e.g. the modified betatron),[3,4] where the electric field is continuous along the beam orbit. The cyclic accelerators have the advantage of compactness. However, they have the disadvantage that it takes several thousand revolutions of the beam to acquire an energy that is gained in a single pass of the accelerating gap of a linear accelerator. Because of the slow acceleration, field errors, instabilities, and radiation losses impose limitations on cyclic accelerators. Therefore, a device that combines the rapid acceleration of linear accelerators and the compactness of cyclic accelerators would be desirable.

A general method to achieve this is to recirculate the electron beam through an accelerating module. BRL has been engaged in studying various recirculating schemes[5] since 1978, when Eccleshall et al.[6] showed that it is theoretically possible to transfer 100 percent of energy of charged transmission lines to an appropriately impedance mismatched electron beam pulse that is recirculated in phase with the accelerating waveform.

There are two distinct classes of beam recirculation schemes: those that utilize ion focusing by a low pressured gas and those that use magnetic fields. This report is concerned with schemes that rely solely on magnetic fields for beam confinement and for guidance in a vacuum.

High current recirculating accelerator concepts that use strong focusing magnetic fields, in addition to any other magnetic fields, may be conveniently called "strong focused recirculating accelerators" (SFRA). In these devices, the strong focusing magnetic field is produced by current carrying helical windings of the stellarator/torsatron type. One such accelerator concept, jointly developed by BRL and the Naval Research Laboratory (NRL), has been referred to as the rebatron.[7-9] It is directly related to some of the other SFRA concepts: the stellatron,[10] RIA,[11] and SLIA.[12]

In this report we present a beam envelope analysis for application to high-current, strong focusing accelerators in general and to SLIA and rebatron in particular. We then describe the rebatron and the beam dynamics of its acceleration to analyze a beam injection scheme for the rebatron.

II. AN ANALYSIS OF BEAM ENVELOPE IN STELLARATOR FIELDS

High-current, strong focusing accelerators typically rely on a $\ell = 2$ (or other multipole) stellarator/torsatron magnetic field, in addition to a longitudinal magnetic field, for beam confinement. The stellarator field is produced by 2ℓ helically wound wires with currents flowing in opposite directions in the neighboring wires.

The $\ell = 2$ stellarator field requires four wires. The $\ell = 2$ torsatron field can be generated by two helically wound wires with currents flowing in the same direction. In either case, a strong-focusing transverse field and a zero-order longitudinal field is produced. The field produced can be called a rotating quadrupole field.

For a continuously rotating quadrupole field, in the approximation when only the lowest power in r of the focusing field is included, the radii of an elliptical K-V distribution beam were first analyzed by Gluckstern[13] for a straight transport line. In a similar way, the $\ell = 2$ stellarator type beams have also been analyzed for weak stellarator fields[12,14] together with a longitudinal field. Our analysis is carried out without any restrictions on r or on the strength of the stellarator focusing field. Our treatment is in the spirit of a general formulation for beam envelope.[15] For simplicity, we will here develop the specialized beam envelope equation for the laminar flow of a cold beam of uniform density in a straight section.

A. Proof of a Constant of Motion.

Even without scattering, the canonical angular momentum is not conserved because of the presence of the non-axially symmetric helical field. However, we have derived another constant of motion. In cylindrical coordinates (r, ϕ, z), the externally applied field, being helically symmetric, can be written as a

function of r and $\psi = \phi - z/\mu$, where $\mu = L/2\pi = 1/\alpha$, and L is the pitch of the helix:

$$B_r^e = 2\, b_2\, I_2'\,(2r/\mu)\, \sin 2\psi \tag{1}$$

$$B_\phi^e = \frac{\mu}{r}\, 2\, b_2\, I_2\,(2r/\mu)\, \cos 2\psi \tag{2}$$

$$B_z^e = B_0 - 2b_2\, I_2\,(2r/\mu)\, \cos 2\psi \tag{3}$$

where B_o is the externally applied longitudinal field, b_2 is the strength of $\ell = 2$ stellarator field and I_2 is the modified Bessel function.

The relativistic Lagrangian of a particle of charge q in an electromagnetic field (ϕ, $\vec{A}$)is

$$L = - mc^2 \sqrt{1-\beta^2} - q\,\phi + \frac{q}{c}\,\vec{A}\,.\,\vec{v} \tag{4}$$

where $\beta = \frac{v}{c}$. Now,

$$\frac{\partial L}{\partial \dot{z}} \equiv P_z = \gamma\, m\, v_z + \frac{q}{c}\, A_z \tag{5}$$

and

$$\frac{\partial L}{\partial \dot{\phi}} \equiv P_\phi = r\,(\gamma\, m\, v_\phi + \frac{q}{c}\, A_\phi) \tag{6}$$

where $v_z \equiv \dot{z}$ and $v_\phi = r\,\dot{\phi}$. We can write $\vec{A} = \vec{A}^e + \vec{A}^s$, where the superscripts 'e' and 's' denote external and self-fields, respectively. The external fields, given by Eqs. (1)-(3), possess helical symmetry: they depend on r and $(\phi - z/\mu)$ only. When the $\ell = 2$ stellarator field is added to a uniform longitudinal guide field, the cross-section of the beam would become elliptical rather

than circular. Although the beam does not then possess azimuthal symmetry, it is reasonable to assume that, going along the z-axis, the cross-section ellipse rotates with the externally applied fields, at least for a matched beam, so that the self-fields have the same helical symmetry: $\vec{A}^s = \vec{A}^s(r, \phi - z/\mu)$, $\phi^s = \phi^s(r, \phi - z/\mu)$. Differentiation of Eq. (4) then gives

$$\mu \frac{\partial L}{\partial z} + \frac{\partial L}{\partial \phi} = 0$$

and Lagrange's equations can be combined to give

$$\mu P_z + P_\phi = K = \text{constant} \tag{7}$$

Thus,

$$\frac{q}{c}(\mu A_z^e + r A_\phi^e) + \frac{q}{c}(\mu A_z^s + r A_\phi^s) + \mu \gamma m v_z + \gamma m v_\phi r = K \tag{8}$$

is a constant of the motion.

B. Beam Envelope Equation.

For the external fields given in Eqs. (1)-(3), we find that

$$\mu A_z^e + r A_\phi^e = B_0 \frac{r^2}{2} - \mu r b_2 I_2' \cos 2\psi \quad . \tag{9}$$

Substituting Eq. (9) and the self-fields of the beam of elliptical cross-section into Eq. (8), we obtain, assuming that B_ϕ^s is the dominant magnetic self-field, for a particle at the beam surface

$$v_\phi = (\gamma r)^{-1} \left[\frac{K}{m} - \frac{\Omega}{2} r^2 + \mu r \Omega_2 I_2' \cos 2\psi - \mu \gamma \eta v_z\right] \tag{10}$$

where $\Omega = qB_0/mc$ and $\Omega_2 = qb_2/mc$; $\eta = 1 - \frac{\omega_p^2}{4c^2\gamma} r^2 \left(2 - \frac{r}{r_c}\right)$, $\omega_p^2 = \frac{4\pi nq^2}{m}$

and r_c is the radius of the circular cross-section of the beam when only the longitudinal field, B_0, is applied. Considering particle motion at the beam-edge, substitution of Eq. (10) into the radial component of the transverse equation of motion

$$\ddot{r} + \dot{\gamma}\frac{\dot{r}}{\gamma} - \frac{v_\phi^2}{r} = \frac{e}{\gamma m}\left[E_r + \frac{1}{c}\left(v_\phi B_z - v_\phi B_\phi\right)\right] \tag{11}$$

then leads to the radial envelope equation of a cold (low emittance) beam, for the case of no acceleration ($\dot{\gamma} = 0$), in the paraxial approximation as

$$\ddot{R} + \left(\frac{\Omega}{2\gamma}\right)^2 R - \frac{\omega_p^2}{2\gamma^3} R \left(2 - \frac{R}{r_c}\right) = \frac{(K/m)^2}{\gamma^2 R^3} -$$

$$\frac{2(K/m)}{\gamma^2 R}\left[\left(I_2 - \frac{\mu}{R} I_2'\right)\Omega_2 \cos 2\psi + \frac{\mu\zeta}{R^2}\right] -$$

$$\frac{2\mu}{\gamma^2}\Omega_2 I_2 \cos 2\psi \left[\Omega_2 I_2' \cos 2\psi - \frac{\zeta}{R}\right] + \frac{\mu^2}{\gamma R}\left[\Omega_2 I_2' \cos 2\psi - \frac{\zeta}{R}\right]^2 \tag{12}$$

where $\zeta = \gamma\beta c - \frac{\beta}{c}\frac{\omega_p^2}{4} R^2 \left(2 - \frac{R}{r_c}\right)$.

Equation (12) is the beam envelope equation for the space-charge dominated transport of an electron beam in an $\ell = 2$ stellarator field (e.g., in the straight section of SLIA).[16] In Eq. (12) $\psi = \phi - \alpha z$, where z is the propagation distance along the axis and ϕ is the azimuthal angle. The beam radius R is a function of ϕ and z so that the beam cross-section is a rotating ellipse. The cross-section has become elliptical since, in addition to the externally applied longitudinal field $B_0 = \Omega mc/q$ (produced by solenoidal current windings), there is also the $\ell = 2$ stellarator field $b_2 = \Omega_2 mc/q$. It may be noted that the beam self-fields used in the derivation of Eq. (12) were for a beam with eliptical cross-section. If the stellarator field were turned off, the beam would have a circular radius r_c in the externally applied confining field B_0. In Eq. (12) certain terms have been put in terms of r_c for the sake of convenience, particularly for comparing it with the standard envelope equation for the case when only a parallel external magnetic field is present.[15] Although, in the above derivation, beams of uniform density have been assumed, the change in density resulting from deformation of a circular beam to an elliptical beam has been taken into account. Our beam envelope equation is valid for arbitrary values of R, b_2, and B_0. In these respects, the beam envelope Eq. (12) appears to be an improvement over previous treatments[13,14] of the beam envelope for high current beams in strong focusing configurations.[17]

We note that the beam envelope Eq. (12) reduces to the standard envelope equation for space-charge dominated beam transport (or a beam with negligible emittance) in a parallel (longitudinal) magnetic field when the $\ell = 2$ stellarator field is turned off. In that limiting case, $\Omega_2 \to 0$, $\mu \to 0$; so that by Eq. (7), $K \to P_\phi$ and also $R/r_c \to 1$. Equation (12) then becomes

$$\ddot{R} + \left(\frac{\Omega}{2\gamma}\right)^2 R - \frac{\omega_p^2}{2\gamma^3} R = \frac{(P_\phi/m)^2}{\gamma^2 R^3} \tag{13}$$

III. BEAM ACCELERATION AND INJECTION IN A REBATRON

A. The Rebatron.

The rebatron,[7,8] which is the product of a joint BRL-NRL project, is shown schematically in Fig. 1. As in the linear induction accelerators, the electrons in the rebatron undergo rapid acceleration by transiting through a localized (few centimeters long) inductive accelerating gap. However, in order to achieve the compactness of cyclic accelerators, instead of using a series of accelerating gaps in a linear configuration, the rebatron recirculates the electron beam repeatedly through the same accelerating gap in a closed ring. The accelerating gap produces an energy gain of ~ 2 MeV per pass, and the beam is recirculated in a toroidal pipe of cross-sectional radius 10 cm and major (ring) radius 1 meter. The high-gradient localized electric field that is responsible for the rapid acceleration of electrons is produced by a convoluted parallel transmission line.

Other transmission lines may be used, depending upon the final beam parameters desired. In particular, to achieve moderate energies of ~ 20 MeV for the radiography application, one could use the ET-2, or the Radlac, radial line cavities,[2,6] as shown in Fig. 2.[18]

In the circular geometry shown in Figs. 1 and 2, the applied magnetic fields consist of a toroidal magnetic field, a vertical magnetic field, and an $\ell = 2$ (or other multipole) torsatron field. The difficulty of matching the vertical magnetic field to the electron energy (which, in the rebatron changes by ~ MeV at each successive recirculation of the beam) is overcome by applying the $\ell = 2$ torsatron field, which gives a large bandwidth for mismatch tolerance between electron energy and the vertical field. The beam can thus be made to recirculate through the high-gradient accelerating gap in a single toroidal beam pipe of reasonably small cross-sectional radius (~ 10 cm). The $\ell = 2$ torsatron field can be

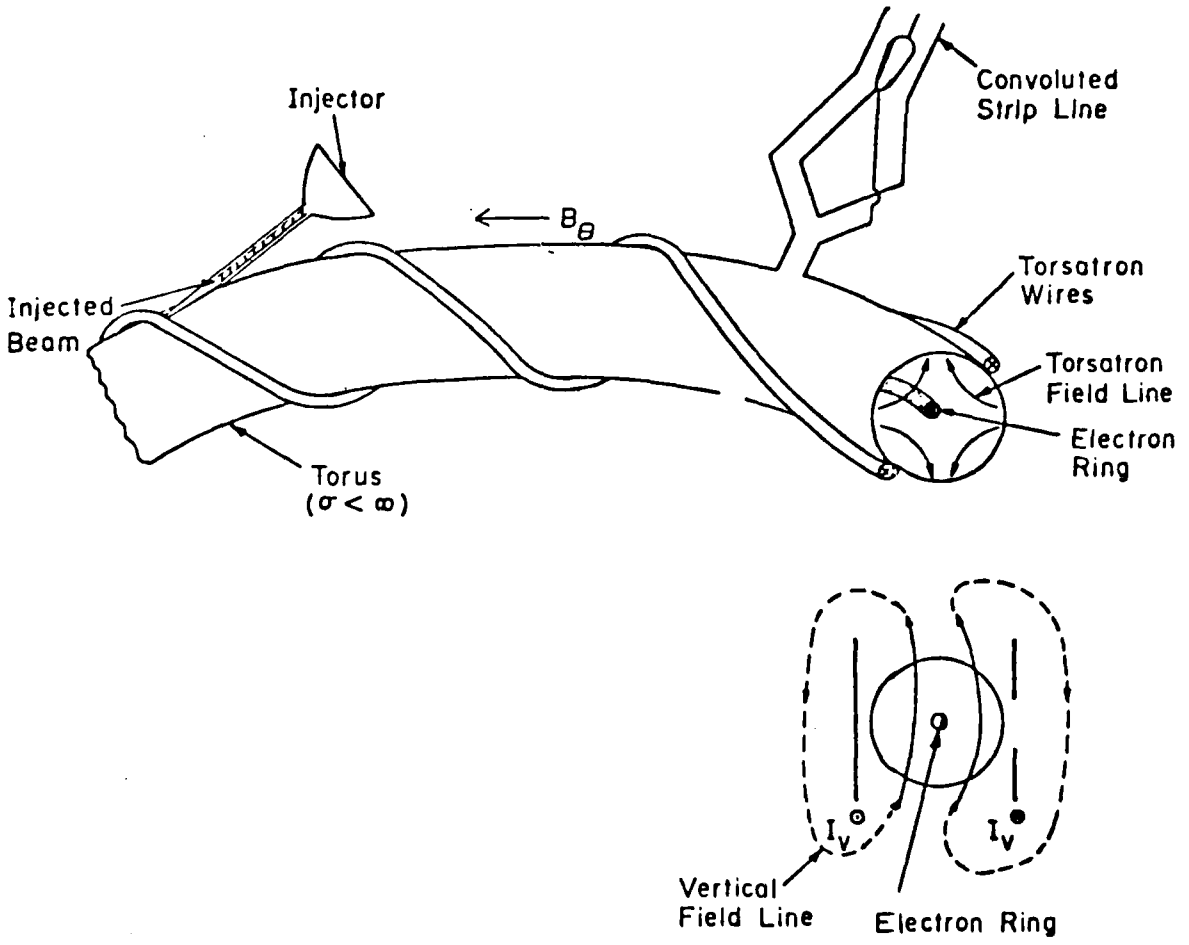

Figure 1. Schematic of a SFRA named "rebatron". Inset at lower right shows low inductance coaxial lines to produce a vertical magnetic field that can be ramped.

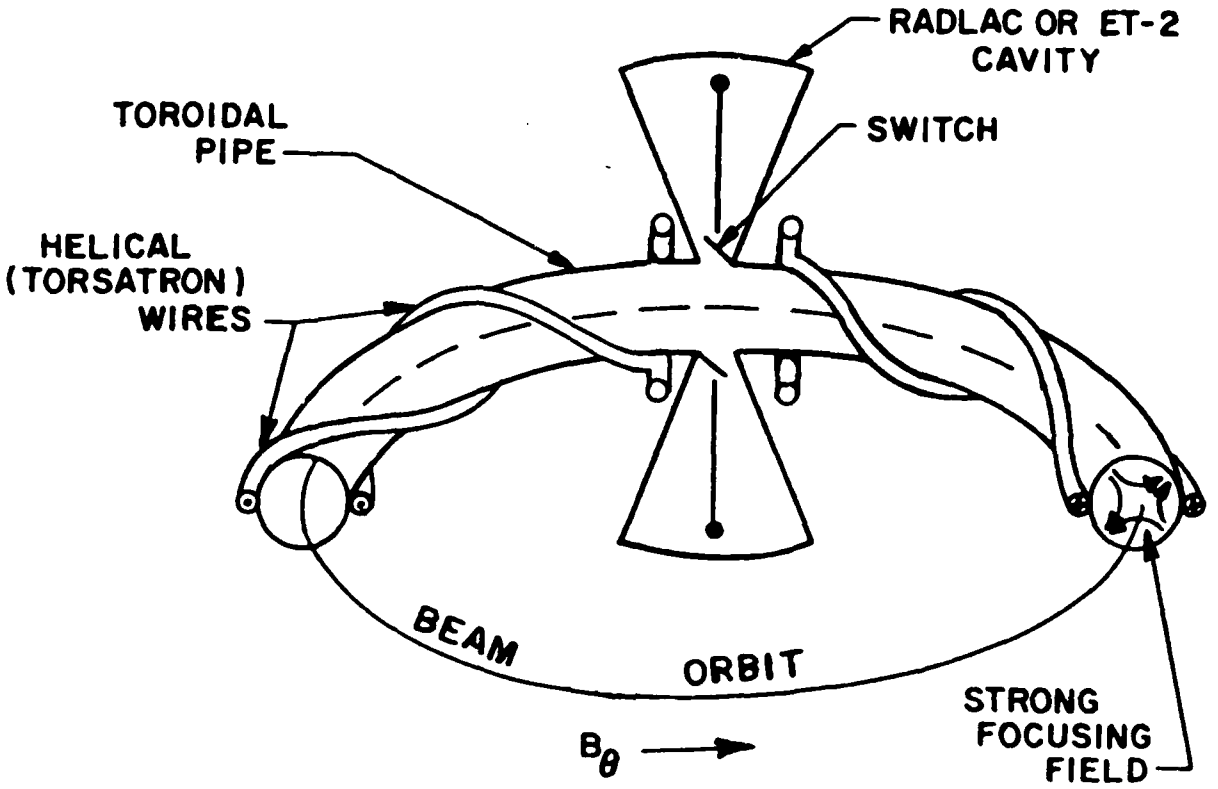

Figure 2. Schematic of the SFRA (strong focused recirculating accelerator) in which radial line/ET-2 cavities are used for producing electric field at the accelerating gap.

generated by two wires wound helically on the torus, the wires carrying currents flowing in the same direction. The helically wound wires generate a twisting strong-focusing transverse magnetic field, as shown by the four curved arrows drawn in the cross-section of the toroidal pipe in Figs. 1 and 2.

The strong-focusing field gives a large tolerance of energy range of the beam that can be turned with a given vertical field, without striking the pipe wall. As a result, the rebatron can produce beams of several tens of MeV even with a fixed vertical field of a few hundred Gauss.[7,8]

To achieve higher energies, the vertical field in the rebatron is increased rapidly in approximate synchronism with beam acceleration. This is accomplished by passing currents in opposite directions through two parallel cylindrical plates, mounted coaxially with the toroidal pipe.[7] This low inductance arrangement is shown in the lower right inset of Fig. 1. The purpose of the gap in the outer plate is to provide a field with the desired field index. Starting with an injection energy of 2.5 MeV, the rebatron can then achieve final energies exceeding 800 MeV with beam currents of tens of kiloamperes.[7,8]

B. Beam Dynamics of Acceleration.

In the local cylindrical coordinate system $\hat{e}_\rho$, $\hat{e}_\phi$, $\hat{e}_s$ shown in Fig. 3, the components of $\ell = 2$ torsatron magnetic field are given by

$$B_\rho = B_\rho^{(0)} + B_\rho^{(1)} + B_\rho^{(1)},$$

$$B_\phi = B_\phi^{(0)} + B_\phi^{(1)} + B_\phi^{(1)},$$

$$B_s = \frac{1}{1 + (\rho/r_0)\cos\phi}\left[B_s^{(0)} + B_s^{(1)} + B_s^{(1)}\right], \qquad (14)$$

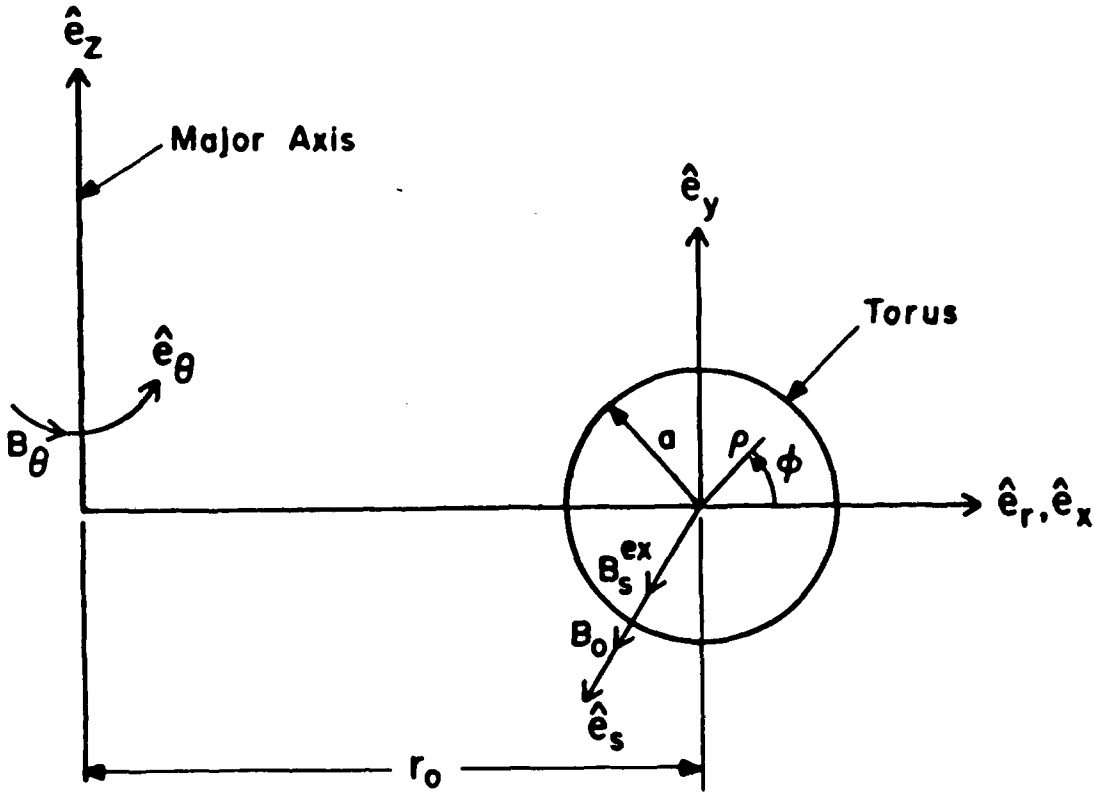

Figure 3. Coordinate system used to study SFRA beam dynamics.

where

$$B_\rho^{(0)} = B_0 \sum_{m=1}^{\infty} A_m^{(0)}\, mx_0 I'_{2m}(mx) \sin\psi$$

$$B_\phi^{(0)} = B_0 \sum_{m=1}^{\infty} A_m^{(0)}\, 2m \frac{x_0}{x} I_{2m}(mx) \cos\psi \qquad (15)$$

$$B_s^{(0)} = B_0 \{1 - \sum_{m=1}^{\infty} A_m^{(0)}\, mx_0 I_{2m}(mx) \cos\psi\}$$

with

$$\psi = 2m(\phi - \alpha s) \qquad (16)$$

are the zero order field components produced by the helical windings in a straight (cylindrical) configuration, and the terms with superscript (1) in Eq. (14) are the first order toroidal corrections, proportional to ρ_0/r_0, and are explicitly given in Ref. 7. The remaining terms are defined as follows:

$$A_m^{(0)} = K'_{2m} (mx_0) C_m$$

$$C_m = \frac{2 \sin 2 m \delta}{2 m \delta}$$

$$B_0 = \frac{8\pi I}{cL}$$

$$x_0 = 2 \alpha \rho_0$$

$$x = 2 \alpha \rho$$

$$\alpha = \frac{2\pi}{L}$$

where I is the current flowing in the windings; $2\delta\rho_0$ is the width of the current carrying conductor; r_0 is the major radius of the torus; and $I_n(x)$, $K_n(x)$, $I'_n(x)$ and $K'_n(x)$ are the Bessel functions and their derivatives. In a toroidal device, the period should satisfy the relation $2\pi r_0/L = N$ where N is an integer. In addition to the torsatron field, the rebatron accelerator includes a "betatron" or vertical magnetic field described by the linearized equations

$$B_z = B_{z0} [1 - nx/r_0] \tag{17}$$

$$B_r = - B_{z0} ny/r_0 \tag{18}$$

where B_{z0} is the betatron field at the reference orbit, at $x = y = 0$, and n is the external field index. The first two non-zero terms in the expansions describe the field for $\rho / \rho_0 < 0.5$ to better than 95 percent accuracy.

The relativistic equations of motion were numerically integrated, using Eqs. (14)-(18) with an accelerating gap 2 cm wide and the electric field limited to a 0.6 radian wide toroidal sector.[7,8] The accelerating voltage was taken as 2 MeV. An external toroidal field $B_s^{ex} = -6$ kG was also applied in addition to the field generated by the torsatron windings. Fig. 4(a) shows the electron energy (γ) as a function of time, and Fig. 4(b) shows the orbit projected on the minor cross-section of the torus, when the current in the torsatron windings is taken to be -250 kA, so that the torsatron field strength factor ε_t is -0.8, where $B_s^{ex}\varepsilon_t = B_0 x_0 K_2'(x_0)$. The betatron field was held constant at 118 G with n = 0.50. Torus major radius was 100 cm and the toroidal chamber minor radius was a = 10 cm, while the winding minor radius was $\rho_0 = 12$ cm. The parameter α was taken as 0.1 cm^{-1}, so that N = 10. The injection energy was $\gamma = 7$, the matching energy for $B_{z0} = 118$ G. It is seen that the particle remains confined for over 14 recirculations and attains γ of approximately 65 before it hits the chamber wall. The total time the electron remains in the system is an order of magnitude greater than when the torsatron field is absent, demonstrating the substantial improvement of confining properties of the system by the addition of a torsatron field.

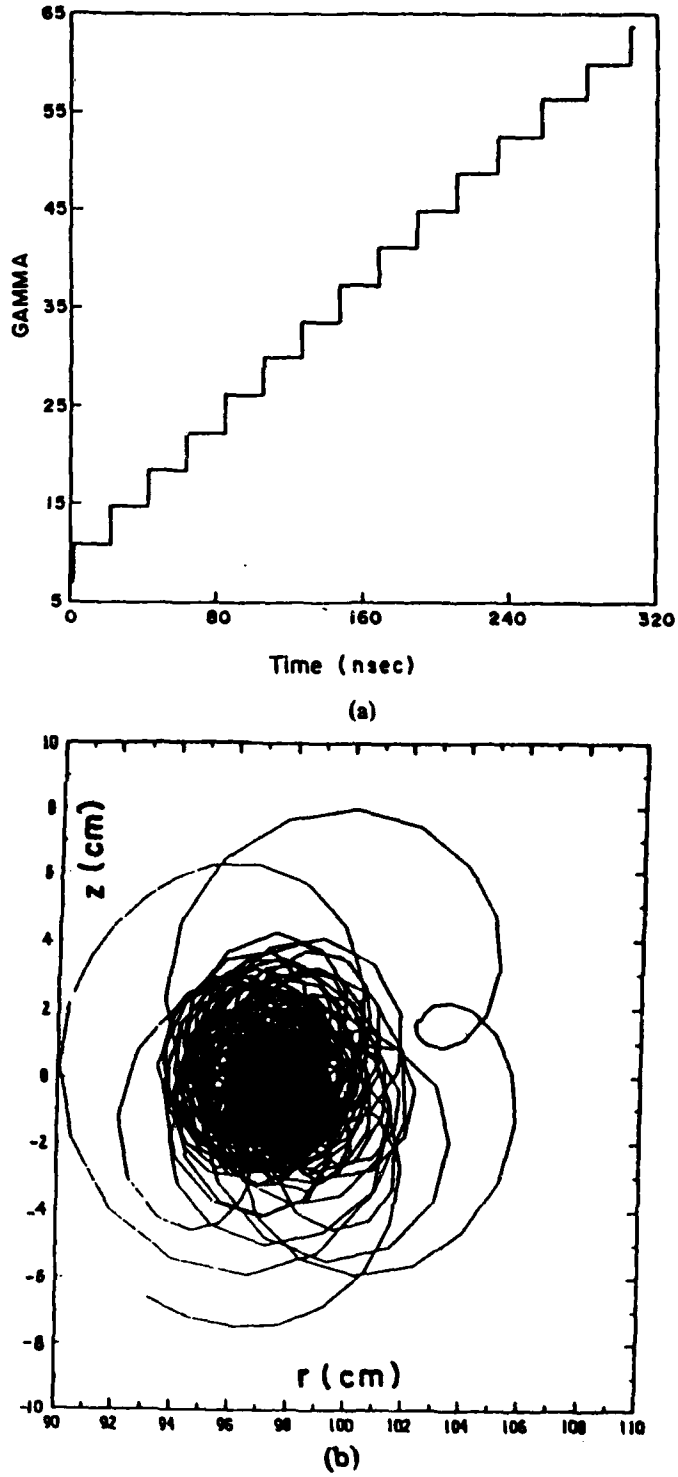

Figure 4. (a) Electron energy [$\gamma \simeq 2$ E (MeV)] as a function of time and (b) the corresponding particle orbit in the (r,z) plane, when the vertical field is held constant at 118 G, in the SFRA shown in Figure 2.

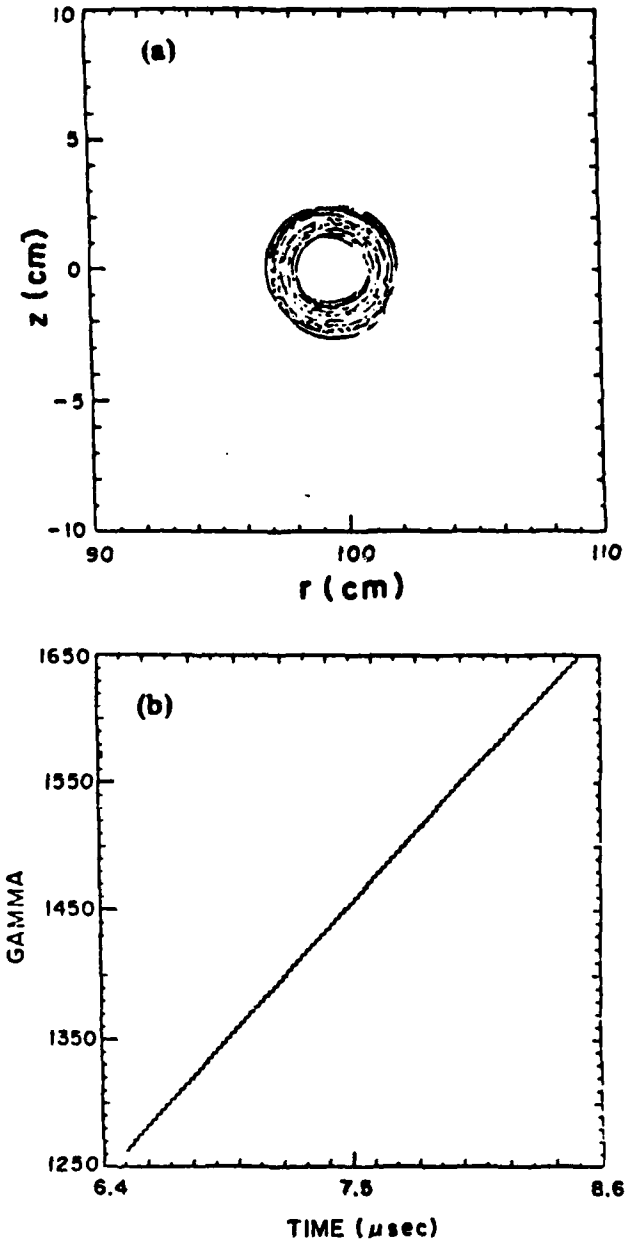

Figure 5. (a) Particle orbit in the transverse plane and (b) particle energy [$\gamma = 2E$ (MeV)] as function of time in a rebatron, which has a rapidly increasing vertical field.

To achieve very high energies ($\gtrsim$1 GeV), the fixed betatron field is replaced by a local vertical magnetic field that varies rapidly with time.[7,8] The synchronism of the vertical field with the electron energy need not be exact (because of the large bandwidth resulting from the torsatron windings) until γ approaches a value for which the matched vertical field equals in magnitude the torsatron field. The rapidly varying vertical field can be generated by two coaxial, cylindrical lines that carry current in the opposite directions and that are concentric with the torus. (See inset, Fig. 1.) By splitting the outer line into two, as shown, the index of the vertical field can be controlled.[7] With such an arrangement, one is able to attain a γ of 1,650 in computer simulations (with a rapid increase of the applied vertical field to approximately 28 kG). Figures 5(a) and (b) show the orbit of an electron in the transverse plane and the increase in γ as a function of time for this high energy mode of the rebatron with torus major radius of 100 cm.[7,8]

C. Beam Dynamics of Injection.

Since the strong focusing magnetic fields in the rebatron make the particle orbits relatively insensitive to energy mismatch, a special scheme is needed to trap a beam near the center of the toroidal ring after it has been injected near the wall. Following NRL's beam trapping scheme for stellatrons,[19] one can accomplish the required shift of the beam position, from near the wall to the minor axis of the torus in a rebatron, by superposing a rapidly varying vertical trapping field, before the rebatron acceleration gap is activated. The beam can then be made to pass through the center of the toroidal cross-section within a few bounce periods. The trapping field is of the form

$$B = \begin{cases} B_0^t \, e^{-(t-t_0)/\tau} & \text{for } t \geq t_0 \ , \\ B_0^t & \text{for } t \geq t_0 \ . \end{cases}$$

The computer simulation of Fig. 6 shows the success of this scheme. In this case, the major radius of the torus was 100 cm and the minor radius was 16 cm. The magnitude of the external toroidal field was 3 kG and the torsatron ($\ell = 2$) field strength had a magnitude of 1 kG. There is also a fixed vertical field of 105 G and index n = 0.5. The beam current is 10 kA and the beam radius is 1 cm. The beam is injected 14 cm away from the minor axis. The trapping is initiated at $t_0 = 10^{-8}$ s, with $\tau = 10^{-7}$ s and $B_0^t = 52$ G. We see that the beam drifts to locations near the minor axis in 2-3 bounces. The rebatron acceleration gap would be appropriately timed to be activated sometime after this drift.

In the example of Fig. 6, the injection energy was $\gamma \simeq 3$. Because of wall effects, as the beam drifts toward the minor axis, it loses energy. The variation of beam energy (as it bounces inward) as a function of time after injection is shown in Fig. 7.

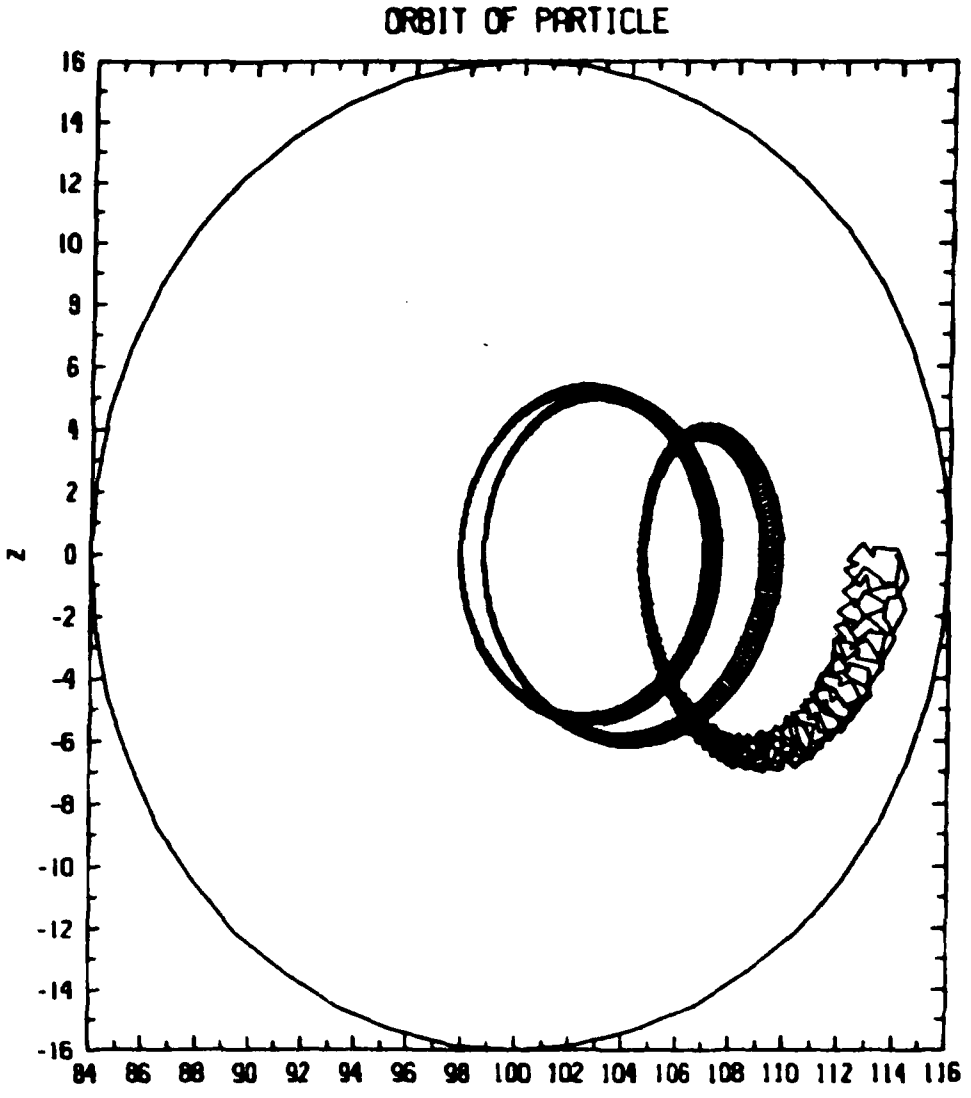

Figure 6. Beam injected near the pipe wall (r = 114 cm) in a rebatron is brought to the center of the pipe (r = 100 cm) by applying a trapping field at injection.

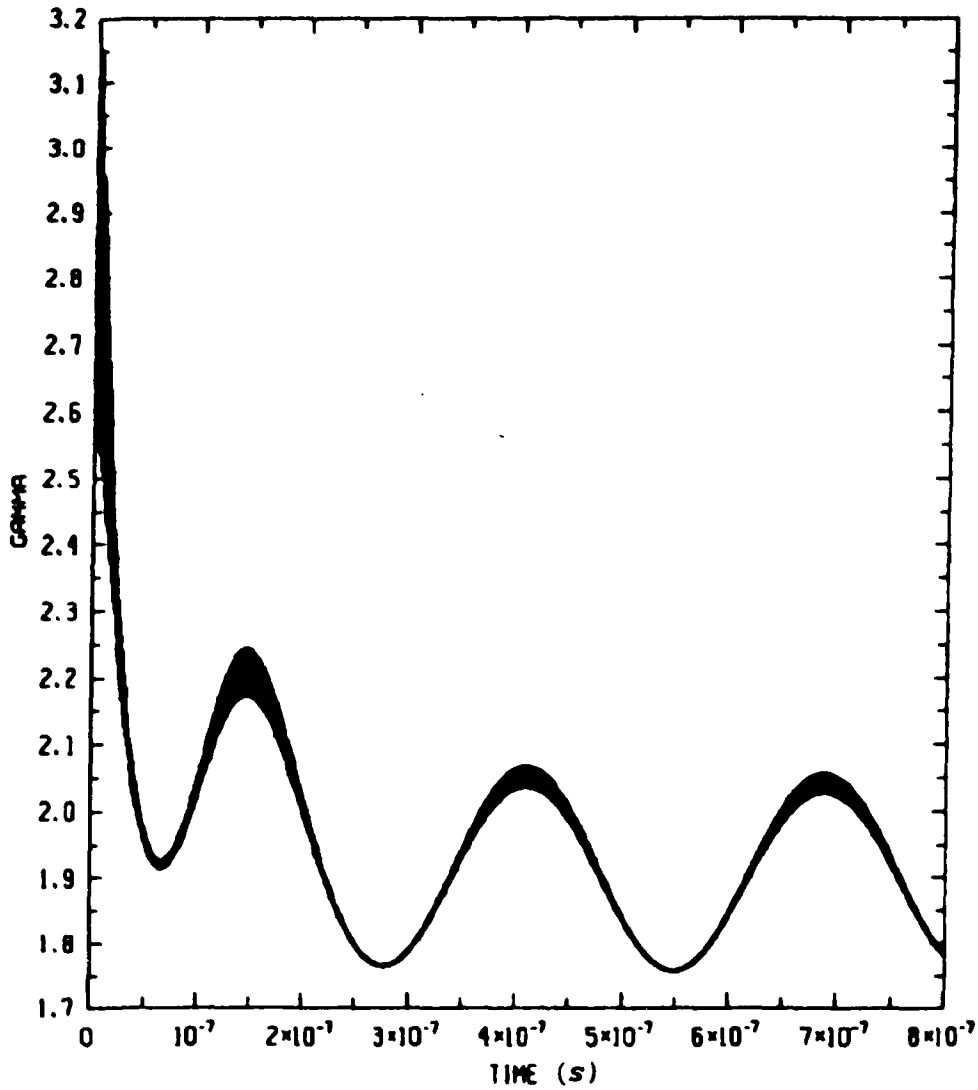

Figure 7. Variation of beam γ as a function of time after injection as the beam bounces toward the minor axis after injection near the wall for the case shown in Fig. 6.

IV. SUMMARY AND CONCLUSIONS

High current electron beam accelerators have a wide range of potential defense and non-defense applications. Induction accelerators, being inherently low impedance devices, are naturally suited to drive high-current beams. There are two generic types of high-current induction accelerators: linear and cyclic. Cyclic accelerators, like the betatron and its various modifications, have the advantage of compactness. However, they have the disadvantage that it takes several thousand revolutions of the beam to acquire an energy, which is gained in a single pass of a linear accelerator. Field errors, instabilities, and radiation losses, therefore, impose limitations on these accelerators. Devices that combine the rapid acceleration of linear accelerators and compactness of cyclic accelerators would be desirable. A general method to achieve this is to recirculate the electron beam through an accelerating module. Since this involves a 360° turn, application of a vertical magnetic field is required. This immediately raises the problem of beam loss due to energy mismatch. This problem can be alleviated by applying a strong-focusing magnetic field, produced by using stellarator (current) windings [10,11] or torsatron windings, [7,8,9] in combination with a toroidal magnetic field. All high current recirculating accelerators that use strong focusing may be conveniently called "strong focused recirculating accelerators" (SFRA). The RIA, [11] SLIA [12] and rebatron [7,8] are examples of SFRA. (The periodic focusing betatron of the University of New Mexico [20] and the MEBA [21] do not come under the category of SFRA.)

An analysis of beam dynamics for SFRA is presented in this report. We have shown that, even though the canonical angular momentum is not conserved because of the presence of non-axially symmetric strong focusing field, there exists a constant of the motion $K = \mu P_z + P_\phi$, where $\mu = 1/\alpha = L/2\pi$, at least for a matched beam (of rotating elliptical cross-section) when toroidal effects are negligible, even when the self-fields are taken into account. This constant of the motion is then used to derive a differential

equation of the radial envelope of a high current electron beam for beam transport, when a strong focusing stellarator magnetic field is applied in addition to a parallel (longitudinal) magnetic field for beam confinement. Unlike some of the other treatments of beam envelope for SFRA, our beam envelope equation, Eq. (12), is not restricted to small values of (x, y) or to weak relative strength of the stellarator field. We also show that our equation reduces to the standard (e.g., Lee and Cooper[15]) beam envelope equation for space-charge dominated beam transport in a parallel (longitudinal) magnetic field when the stellarator field is turned off. Equation (12) is expected to be particularly useful in the design and analysis of SLIA.

Next, a summary description of beam dynamics in another SFRA, the rebatron,[7-9] is given. The rebatron uses two twisted wires, instead of the four used in RIA and stellatron, to generate an $\ell = 2$ strong focusing field, in addition to a parallel (longitudinal) magnetic field (produced by solenoidal windings) and a vertical "betatron" field of suitable index, for recirculating the beam through a localized gap. It is seen that the increased energy bandwidth achieved by such a configuration enables acceleration of beams to tens of MeV with a fixed vertical "betatron" field. The high-gradient localized electric field of the acceleration gap can be produced by Radlac or ET-2 cavities. Assuming an accelerating voltage of 2 MeV per pass and a fixed vertical field of 118 G, the electrons remained confined for more than 14 revolutions to attain a γ of 65 before hitting the wall. For this computer simulation, the currents in the torsatron windings were 250 kA. To achieve higher energies, the vertical field must be ramped. In that case, energies approaching 1 GeV, with beam currents of a few kA, could be theoretically achieved. However, further stability analyses are required to establish the practical potential of such a device. (See, e.g., Ref. 22.)

Since the strong-focusing magnetic fields in the rebatron make the particle orbits relatively insensitive to energy mismatch, a special scheme is needed to trap a beam near the center of the toroidal ring after it has been injected near the wall. Following NRL's beam trapping scheme for stellatrons,[19] this can be accomplished by superposing a rapidly varying vertical trapping field, before the rebatron acceleration gap is activated. It is shown here that this scheme would work for a 10 kA beam of 1 cm radius, injected near the wall of a rebatron torus of major radius 100 cm and minor radius 16 cm, when the magnitudes of the toroidal ("longitudinal") field and the $\ell = 2$ torsatron field are 3 kG and 2 kG, respectively, and a trapping field of magnitude 52 G, with a decay time of 10^{-7}s is applied. The beam would reach the center of the chamber in 2-3 bounces. Thereafter, the localized electric field in the acceleration gap can be suitably activated.

Stability analyses and engineering design studies of rebatron would be needed before a prototype can be built.

REFERENCES

1. Briggs, R.J., Birx, D.L. Caporaso, G.J., Fessenden, T.J. Hester, R.E., Melendes, R., Neil, V.K., Paul, A.C. and Struve, K.W., IEEE Trans. on Nucl Sci., NS-28, No. 3, 3360-64, (1981).

2. Miller, R.B., IEEE Trans. Nucl. Sci., NS-32, 3149 (1985).

3. Sprangle, P. and Kapetanakos, C.A., J. Appl. Phys. 49, 1 (1978).

4. Rostoker, N., Comments on Plasma Physics, Vol. 6, p. 91 (1980); Ishizuka, H., Lindley, G., Mandelbaum, B., Fisher, A., and Rostoker, N., Phys. Rev. Lett. 53, 266 (1984).

5. Frost, C. A., Shope, S. L., Miller, R. B., Leifeste, G. T., Crist, C. E., and Reinstra, W. W., IEEE Trans. Nucl. Sci. NS-32, 2754 (1985); Shope, S. L., Frost, C. A., Leifeste, G. T., Crist, C. E., Kielk, P. D., Poukey, J. W., and Godfrey, R. B., IEEE Trans. Nucl. Sci. NS-32, 3092 (1985); Miller, R.B., IEEE Trans. Nucl. Sci., NS-32, pp. 3152-53 (1980) and citations therein; Siambis, J., IEEE Trans. on Nucl. Sci., NS-30, 3195 (1983).

6. Eccleshall, D. and Temperley, J., J. Appl. Phys. Vol. 49, p. 3649-55 (1978), and references therein.

7. Kapetanakos, C.A., Sprangle, P., Marsh, S.J., Dialetis, D., Agritellis, C. and Prakash, A., Particle Accelerators, Vol. 18, pp. 73-99, (1985).

8. Prakash, A., Marsh, S.J. Dialetis, D., Agritellis, C., Sprangle, P. and Kapetanakos, C.A., IEEE Trans. on Nucl. Sci. NS-32, No. 5, pp. 3265-67 (1985).

9. Kapetanakos, C.A., Sprangle, P., Marsh, S.J., Dialetis, D., Agritellis, C. and Prakash, A., NRL Memo Report No. 5506, (1985).

10. Roberson, C., Mondelli, A. and Chernin, D., Phys. Rev. Lett. 50, 507 (1983); Part. Accel. Vol. 17, 79 (1985); Proc. Fifth Intl. Conf. on High-Power Particle Beams (San Francisco, 1983), p. 442; Ishizuka, H., Leslie, G., Mandelbaum, B., Fisher, A. and Rostoker, N., IEEE Trans. Nucl. Sci. NS-32, 2727 (1985).

11. Mondelli, A. and Roberson, C., Part. Accel., Vol. 15, 221 (1984); IEEE Trans. on Nucl. Sci., NS-30, 3212 (1983).

12. Mondelli, A., Chernin, D.P., Putnam, S.D., Schlitt, L. and Bailey, V., Proc. Beams '86, (in press); see also Ref. 17.

13. Gluckstern, R.L., Proc. 1979 Linear Accelerator Conference, BNL-51134, 245 (1979).

14. Chernin, D., IEEE Trans. on Nucl. Sci., NS-32, 2405 (1985).

15. Lee, E.P. and Cooper, R.K., Part. Accel., Vol. 7, 83 (1976).

16. Prakash, A., Proc. of the 1987 IEEE Particle Accelerator Conference, 16-17 March 1987 (IEEE Catalog No. 87CH2387-9), Vol. 2, pp. 923-924 (1987).

17. Putnam, S.D., Proc. of the 1987 IEEE Particle Accelerator Conference, 16-17 March 1987 (IEEE Catalog No. 87CH2387-9), Vol. 2, pp. 887-891 (1987); Bailey, V., Schlitt, L., Tiefenback, M., Putnam, S., Mondelli, A., Chernin, D., and Petello, J., Proc. of the 1987 IEEE Particle Accelerator Conference, 16-17 March 1987, Vol. 2, pp. 920-922 (1987).

18. Prakash, A., Marsh, S.J., Dialetis, D., Agritellis, C., Sprangle, P. and Kapetanakos, C., IEEE Conference Record (Catalog No. 85CH2199-8), p. 46, June 1985.

19. Kapetanakos, C.A. and Marsh, S.J., (private communication).

20. Humphries, S., Jr., and Len, L.K., Proc. of the 1987 IEEE Particle Accelerator Conference (IEEE Catalog No. 87CH2387-9), Vol. 2, pp. 914-916, (1987).

21. Fisher, A., Rostoker, N., Pearlman, J., and Witham, K., IEEE Trans. on Nucl. Sci., NS-32, 3048 (1985).

22. Godfrey, B.B. and Hughes, T.P., "Quadrupole-Focusing Instability Growth Rate Expressions," (to be published).

(U) DISTRIBUTION LIST

No. of Copies	Organization
2	Administrator Defense Technical Info Center ATTN: DTIC-FDAC Cameron Station, Bldg 5 Alexandria, VA 22304-6145
1	HQDA DAMA-ART-M Washington, DC 20310
1	HQDA (DAMA-CSM-CS) Washington, DC 20310
10	Central Intelligence Agency Office of Central Reference Dissemination Branch Room GE-47, HQS Washington, DC 20505
1	Central Intelligence Agency ATTN: Dr. Jose F. Pina OSWR PO Box 1925 Washington, DC 20013
2	Director Defense Adv Res Projects Agency ATTN: Dr. Lee Buchanan Dr. Shen Shey 1400 Wilson Blvd Arlington, VA 22209
1	Commander US Army Foreign Sci & Tech Cntr ATTN: Dr. Thomas Caldwell 220 Seventh Street, NE Charlottesville, VA 22901
3	Commander US Army Laboratory Command ATTN: R. Vitali, Tech Director Dr. R. Odom, AMSLC-AS-SE Dr. John Rosado, SLCHD-RT 2800 Powder Mill Road Adelphi, MD 20783
2	Commander US Army Training & Doctrine Command ATTN: ATCD-TA, Dr. M. Pastel ATCE-ML, Mr. J. Gray Fort Monroe, VA 23651
1	Commander US Army Material Command ATTN: AMCDRA-ST 5001 Eisenhower Avenue Alexandria, VA 22333
3	Commander US Army Combined Arms Center ATTN: ATZL-CAM - D. E. Skelton ATZL-CAM-D - CPT Kienke ATZL-SCI - Dr. James Fox Fort Leavenworth, KS 66027
1	Commander US Army Dev & Employment Agency ATTN: MODE-ORO Fort Lewis, WA 98433-5000
1	Commander US Army Missile Command Res Dev & Engineering Center ATTN: AMSMI-RD Redstone Arsenal, AL 35898
1	Director US Army Strategic Defense Command ATTN: DASD-H-WD-P PO Box 1500 Huntsville, AL 35807
1	Commander US Army Strategic Defense Command ATTN: DASP-DP (Major Barton Clare) PO Box 15280 Arlington, VA 22205-0150
1	Commander US Army Missile & Space Intelligence Center ATTN: AMSMI-YDL Redstone Arsenal, AL 35898-5500

(U) DISTRIBUTION LIST

No. of Copies	Organization
1	Commander US Army Tank Automotive Command ATTN: AMSTA-TSL Warren, MI 48297-5000
1	Commander US Army Research Office ATTN: Dr. R. Lontz PO Box 12211 Research Triangle Park, NC 27709
1	Director US Army TRADOC Systems Analysis Center ATTN: ATOR-TSL White Sands Missile Range, NM 88002-5502
1	Commander US Army Armament, Munitions & Chemical Command ATTN: AMSMC-ESP-L Rock Island, IL 61299-7300
1	Director US Army AMCCOM ARDEC CCAC Benet Weapons Lab ATTN: SMCAR-LCB-TL Watervliet, NY 12189-4050
5	SDIO Office of Secretary of Defense ATTN: LTC R. L. Gullickson (DEWO) LTC W. Higgins (DEWO) Dr. D. Dustin (IST) Dr. L. C. Marquet (DEWO) COL C. T. Meyer (DEWO) The Pentagon Washington, DC 20301-7100
1	Commander ERADCOM Technical Library ATTN: DELSD-L (Rpt Section) Fort Monmouth, NJ 07703-5301
1	Commander US Army ARDEC ATTN: SMCAR-TDC Dover, NJ 07801

No. of Copies	Organization
1	Commander US Army AMCCOM Armament R&D Center ATTN: SMCAR-MSI Dover, NJ 07801-5001
1	Commandant US Army Infantry School ATTN: ATSH-CD-CSO-OR Fort Benning, GA 31905-5400
1	NVEOC ATTN: AMSEL-CT-L Dr. R. Rohde Fort Belvoir, VA 22060
1	Commander US Army Aviation R&D Command ATTN: AMSAV-E 4300 Goodfellow Blvd St. Louis, MO 63120
1	Director US Army Air Mobility R&D Lab Ames Research Center Moffett Field, CA 94035
1	Commander US Army Communications - Electronics Command ATTN: AMSEL-ED Fort Monmouth, NJ 07703-5000
1	President US Army Armor & Engineer Board ATTN: ATZK-AE-TD - Mr. W. Wells Fort Knox, KY 40121-5470
4	Commander Naval Surface Weapons Center ATTN: Code H23, Dr. E. Nolting Code R41, Dr. M. H. Cha Code R41, Dr. Han S. Uhm Code R401, Dr. Bertram Hui White Oak Silver, Spring, MD 20902-5000

(U) DISTRIBUTION LIST

No. of Copies	Organization
7	Naval Research Laboratory ATTN: Code 4790 - Dr. P. Sprangle Dr. S. J. Marsh Dr. M. Lampe Dr. G. Joyce Dr. R. Hubbard Code 4750 - Dr. R. Meger Code 4710 - Dr. C. Kapetanakos 4555 Overlook Avenue, SW Washington, DC 20375-5000
1	Office of Naval Research ATTN: Dr. C. W. Roberson 800 N. Quincy Street Arlington, VA 22217
1	Commander Space & Naval Warfare Systems Command ATTN: LTCDR W. Fritchie, PMW-145 Washington, DC 20363-5100
1	AFWL/NTYP ATTN: Dr. W. L. Baker Air Force Weapons Laboratory Kirtland AFB, NM 87117
1	AFWL/SUL Kirtland AFB, NM 87117
1	Air Force Armament Laboratory ATTN: AFATL/DOIL (Tech Info Cntr) Eglin AFB, FL 32542-5438
1	AF Ofc of Scientific Research ATTN: Dr. Hugo Weichel Dir, Physical & Geophysical Sciences Bolling AFB Washington, DC 20332
1	USAF Foreign Tech Div ATTN: HQ FTD/TOTD Mr. C. J. Butler Wright-Patterson AFB, OH 45433
1	AFELM, The Rand Corporation ATTN: Library-D PO Box 2138 Sante Monica, Ca 90401-2138
1	La Jolla Institute ATTN: Dr. Keith Brueckner PO Box 1434 La Jolla, CA 92038
1	Rand Corporation ATTN: Dr. S. Kassel 2100 M Street, NW Washington, DC 20037
11	Director Lawrence Livermore National Lab ATTN: L-626, Dr. W. A. Barletta Dr. R. C. Briggs Dr. A. C. Smith, Jr. Jr. Dr. Hans Kruger Dr. W. M. Fawley Dr. Simon S. Yu Dr. G. J. Caporaso Dr. F. W. Chambers Dr. J. K. Boyd Dr. D. S. Prono L-477, Dr. J. Mark PO Box 808 Livermore, CA 94550
10	Sandia National Laboratory ATTN: Dr. J. P. VanDevender, 1200 Dr. D. Hasti, 1243 Dr. K. Prestwich, 1240 Dr. C. A. Frost, 1272 Dr. John Freeman 1241 Dr. S. L. Shope, 1272 Dr. M. G. Mazarakis, 1272 Dr. J. W. Poukey Dr. James Rice Albuquerque, NM 87185
1	Los Alamos National Laboratory International Technology Div ATTN: Dr. E. Kutyreff PO Box 503 Los Alamos, NM 87544

(U) DISTRIBUTION LIST

No. of Copies	Organization
3	Los Alamos National Laboratory ATTN: Dr. Joseph Mack Dr. T. P. Starke Dr. Carl Ekdahl PO Box 1663 Los Alamos, NM 87545
1	MIT Lincoln Laboratory ATTN: Dr. J. Lipsitiz PO Box 73 Lexington, MA 02173-0073
1	Science Applications Int. Corp. ATTN: Dr. A. Armstrong PO Box 2351 La Jolla, CA 92037
4	Science Applications Int. Corp. ATTN: Dr. A. Drobot Dr. A. Mondelli Dr. D. Chernin Dr. W. W. Rienstra 1710 Goodridge Drive McLean, VA 22102
1	Science Applications Int. Corp. ATTN: Dr. R. Johnston 5150 El Camino Real, Suite B-31 Los Altos, CA 94022
1	SRI International ATTN: Dr. Donald J. Eckstrom PSO-25 Molecular Physics Lab 333 Ravenswood Avenue Menlo Park, CA 94025
1	Spectra Technology ATTN: Dr. Dennis Lowenthal 2755 Northup Way Bellevue, WA 98004
1	Lockhead Missiles & Space Co., Inc. Applied Physics Laboratory ATTN: Dr. J. Siambis 3251 Hanover Street Palo Alto, CA 94304
1	Titan/Spectron, Inc. Attn: R. Bruce Miller PO Box 4399 Albuquerque, NM 87196
1	Directed Technologies, Inc. ATTN: Dr. Nancy Chesser 8500 Leesburg Pike, Suite 601 Vienna, VA 22180
1	Titan Systems, Inc. ATTN: Dr. R. Michael Dowe, Jr. 9191 Towne Centre Drive, Suite 500 San Diego, CA 92122
1	Mission Research Corporation ATTN: Dr. Brendan Godfrey 1720 Randolph RD, SE Albuquerque, NM 87106
1	ORI, Inc. ATTN: Dr. Charles M. Huddleston 1375 Picard Drive Rockville, MD 20850
4	Pulse Sciences Inc. ATTN: Dr. Sidney D. Putnam Dr. V. Bailey Dr. L. Schlitt Dr. M. Tiefenback 600 McCormick Street San Leandro, CA 94577
1	Maxwell Laboratories ATTN: Dr. K. Witham 8888 Balboa Avenue San Diego, CA 92123
1	Westinghouse Electric Corporation ATTN: Dr. M. Nahemow 1310 Beutah Road Pittsburgh, PA 15235
1	R.L. Gluckstern Dept. of Physics & Astronomy University of Maryland College Park, MD 20742
1	Dr. N. Rostoker Dept of Physics University of California Irvine, CA 92717

(U) DISTRIBUTION LIST

No. of Copies	Organization
1	Dr. Edward P. Lee Lawrence Berkeley Laboratory Building 47, Room 111 Berkeley, CA 94720
1	Dr. D. Keefe Lawrence Berkeley Laboratory Building 50, Room 149 Berkeley, CA 94720
1	Dr. A. Sessler Lawrence Berkeley Laboratory Building 4, Room 111E Berkeley, CA 9472
1	Dr. Ronald C. Davidson Massachusetts Institute of Technology Cambridge, MA 02139
1	Dr. R. J. Glauber Lyman Laboratory of Physics Harvard University Cambridge, MA 02138
1	Dr. S. Humphries Institute for Accelerator and Plasma Beam Technology University of New Mexico Albuquerque, NM 87131
1	Dr. C. L. Hammer Department of Physics Iowa State University Ames, IA 50011

Aberdeen Proving Ground

Dir, USAMSAA
ATTN: AMSXY-CS (Mr. Phil Beavers)
AMSXY-D
AMSXY-MP, H. Cohen

Cdr, USATECOM
ATTN: AMSTE-TO-F

Cdr, AMCCOM
ATTN: SMCCR-RSP-A
SMCCR-MU
SMCCR-SPS-IL

No. of Copies	Organization
1	Dr. Allen Boozer Dept. of Physics College of William & Mary Williamsburg, VA 23185
1	Dr. Sam Penner 10500 Pine Haven Terrace Rockville, MD 20852
1	Dr. James Leiss 13013 Chestnut Oak Dr. Gaithersburg, MD 20878
1	Dr. J. D. Lawson Rutherford Appleton Laboratory Chilton, Oxon OX11 OQX, U.K.

USER EVALUATION SHEET/CHANGE OF ADDRESS

This Laboratory undertakes a continuing effort to improve the quality of the reports it publishes. Your comments/answers to the items/questions below will aid us in our efforts.

1. BRL Report Number_____ Date of Report_____

2. Date Report Received_____

3. Does this report satisfy a need? (Comment on purpose, related project, or other area of interest for which the report will be used.)_____

4. How specifically, is the report being used? (Information source, design data, procedure, source of ideas, etc.)_____

5. Has the information in this report led to any quantitative savings as far as man-hours or dollars saved, operating costs avoided or efficiencies achieved, etc? If so, please elaborate._____

6. General Comments. What do you think should be changed to improve future reports? (Indicate changes to organization, technical content, format, etc.)

CURRENT ADDRESS

Name

Organization

Address

City, State, Zip

7. If indicating a Change of Address or Address Correction, please provide the New or Correct Address in Block 6 above and the Old or Incorrect address below.

OLD ADDRESS

Name

Organization

Address

City, State, Zip

(Remove this sheet, fold as indicated, staple or tape closed, and mail.)

FOLD HERE

Director
U.S. Army Ballistic Research Laboratory
ATTN: SLCBR-DD-T
Aberdeen Proving Ground, MD 21005-5066

NO POSTAGE
NECESSARY
IF MAILED
IN THE
UNITED STATES

OFFICIAL BUSINESS
PENALTY FOR PRIVATE USE, $300

BUSINESS REPLY MAIL
FIRST CLASS PERMIT NO 12062 WASHINGTON, DC
POSTAGE WILL BE PAID BY DEPARTMENT OF THE ARMY

Director
U.S. Army Ballistic Research Laboratory
ATTN: SLCBR-DD-T
Aberdeen Proving Ground, MD 21005-9989

FOLD HERE